The Journal of Chemical Physics

Distinguishing dynamical features of water inside protein hydration layer: Distribution reveals what is hidden behind the average

Cite as: J. Chem. Phys. **147**, 024901 (2017); https://doi.org/10.1063/1.4990693
Submitted: 15 May 2017 • Accepted: 16 June 2017 • Published Online: 11 July 2017

Saumyak Mukherjee, Sayantan Mondal and Biman Bagchi

AIP Publishing

Distinguishing dynamical features of water inside protein hydration layer: Distribution reveals what is hidden behind the average

Saumyak Mukherjee,[a),b)] Sayantan Mondal,[b),c)] and Biman Bagchi[d)]
Solid State and Structural Chemistry Unit, Indian Institute of Science, Bengaluru 560012, India

(Received 15 May 2017; accepted 16 June 2017; published online 11 July 2017)

Since the pioneering works of Pethig, Grant, and Wüthrich on a protein hydration layer, many studies have been devoted to find out if there are any "general and universal" characteristic features that can distinguish water molecules inside the protein hydration layer from bulk. Given that the surface itself varies from protein to protein, and that each surface facing the water is heterogeneous, search for universal features has been elusive. Here, we perform an atomistic molecular dynamics simulation in order to propose and demonstrate that such defining characteristics can emerge if we look not at average properties but the distribution of relaxation times. We present results of calculations of distributions of residence times and rotational relaxation times for four different protein-water systems and compare them with the same quantities in the bulk. The distributions in the hydration layer are unusually broad and log-normal in nature due to the simultaneous presence of peptide backbones that form weak hydrogen bonds, hydrophobic amino acid side chains that form no hydrogen bond, and charged polar groups that form a strong hydrogen bond with the surrounding water molecules. The broad distribution is responsible for the non-exponential dielectric response and also agrees with large specific heat of the hydration water. Our calculations reveal that while the average time constant is just about 2-3 times larger than that of bulk water, it provides a poor representation of the real behaviour. In particular, the average leads to the erroneous conclusion that water in the hydration layer is bulk-like. However, the observed and calculated lower value of static dielectric constant of hydration layer remained difficult to reconcile with the broad distribution observed in dynamical properties. We offer a plausible explanation of these unique properties. *Published by AIP Publishing.* [http://dx.doi.org/10.1063/1.4990693]

I. INTRODUCTION

A layer of water that surrounds every protein molecule in an aqueous solution plays a central role in the structure, dynamics, and function of the protein.[1–22] An early estimation of the width of the hydration layer came from the rotational correlation time obtained by NMR (and later by dielectric relaxation) measurements of the protein in an aqueous solution. The measured time constant was found to be elongated due to the interaction with the surrounding water molecules. Use of the Debye-Stokes-Einstein relation to reproduce the orientational correlation time demonstrates the need for an addition of ~3 Å to the crystallographic radius of the protein.[23] This 3 Å seemed correct to accommodate one layer of water. This tentative agreement served to foster the view that a protein in an aqueous solution is surrounded by a nearly rigid layer of water molecules (the iceberg model). The landmark work of Wüthrich dispelled this idea to some extent by suggesting that the residence time of a water molecule in the layer should be less than ~300 ps.[17,18]

Even earlier than the reported NMR experiments, Pethig and others studied aqueous protein solutions by using dielectric spectroscopy.[14–16,24] They essentially discovered three components that were considered universal by many, including Mashimo[25,26] who carried out extensive studies in the late 1980s. The three components consist of (i) one bulk water-like around 10 ps, (ii) one at 10 ns or so, attributed to protein rotation, and the third (iii) at around 40 ps. The last one was unexpected and was termed "*delta-dispersion*." This was attributed to the protein hydration layer (PHL).

Much later, the problem was re-visited by employing improved NMR techniques,[27–29] time dependent fluorescence Stokes shift (TDFSS) studies,[12,30,31] and also computer simulation studies.[2,32–34] Recent NMR experiments disagree with the existence of a slow component as obtained in TDFSS experiments.[28,35] *The average time obtained was only 2-3 times slower than that of the bulk value*. On the other hand, recent TDFSS experiments consistently produced a time component that was more than one order of magnitude slower than that in the bulk.[13,30,36–41] Let us first focus on results obtained by NMR experiments. By the very nature of the experimental technique, NMR provides only an average value over all water molecules in the system,[29] which includes both surface and bulk water. One can use the Nuclear Overhauser Effect (NOE) or spin exchange technique to obtain a region specific result but NOE has a low time resolution. Magnetic Relaxation Dispersion (MRD) on the other hand has little or no spatial resolution.[29,35] The inability of NMR to provide either spatial or temporal resolution makes it hard to apply to draw any definite

[a)] E-mail: mukherjee.saumyak50@gmail.com
[b)] S. Mukherjee and S. Mondal contributed equally to this work.
[c)] E-mail: sayantan0510@gmail.com
[d)] Author to whom correspondence should be addressed: profbiman@gmail.com

conclusion. TDFSS on the other hand reported the existence of several slow components, ranging from tens of ps to hundreds of ps.[30,33] However, interpretation of the origin of slow components remains controversial to date. Initial experiments by Bhattacharyya and co-workers revealed the existence of time scales ranging from a few ps to even a few ns.[38] However, these experiments had limited time resolution so missed much of the ultrafast response.

Zewail and co-workers carried out experiments on *subtilisin Carlsberg* and sweet protein *monellin* using exposed amino acid residues (tryptophan) as the natural probe.[30] Because of 160 fs time resolution used in these experiments, they missed both the ultrafast and the slow components but obtained the intermediate time scales. Importantly, they compared their TDFSS results on the protein hydration layer with tryptophan in the bulk. Zewail's experiments find a slow component of 38 ps for *subtilisin Carlsberg* and 16 ps for sweet protein *Monellin* which are absent in bulk water solvation.

Computer simulations, however, have provided mixed results. If one uses single particle rotation and probes the second rank spherical harmonic (as in anisotropic depolarization experiments), then one finds a result in good agreement with NMR, that is, a relaxation time ~2-3 times slower than that of the bulk. On the contrary, if one studies dielectric relaxation or the total moment-moment time correlation function of the first layer,[42] then one obtains a multi-exponential decay with the slowest time that is again an order of magnitude slower than that of the bulk.[42] It is perhaps expected that different experimental techniques would lead to different results and different conclusions. For example, it was pointed out by Hubbard and Wolynes,[43] and also by Ravichandran and Bagchi,[44] that dipolar interaction makes the rank (l) dependence of orientational relaxation non-trivial. The Debye $l(l + 1)$ dependence of the rate of relaxation might not hold.[31]

In an interesting study, Hassanali and Singer pointed out that the amino acid side chains can play an important role in slowing down the solvation dynamics of a probe.[32] When they quenched the motion of the side chains, relaxation became faster. One could imagine that this is a trivial consequence of removing the slow energy component from the side chain charged groups, but a later study showed that the situation was not that simple. In some cases, the relaxation became slower when side chain motion was quenched.[33] Therefore, a more detailed study is needed in a microscopic scale.

The main results of the present work are as follows. (i) Distributions of calculated residence times and rotational relaxation times in the hydration layer for four different protein-water systems are unusually broad. We attribute this to the simultaneous presence of peptide backbones that form weak hydrogen bonds, hydrophobic amino acid side chains that form no hydrogen bond, and charged polar groups that form a strong hydrogen bond with the surrounding water molecules. (ii) Importantly, this unusually broad distribution is responsible for the non-exponential relaxations. (iii) While the average time constant is just about 2-3 times larger than that of bulk water, it is seen to provide a poor representation of the real behaviour. In particular, the average leads to the erroneous conclusion that water in the hydration layer is bulk-like. (iv) The much lower value of the static dielectric constant of the hydration layer remained difficult to reconcile with the broad distribution observed in the dynamical properties. We offer a plausible explanation of these unique properties.

We also discuss the relationship of our result of wide distribution of relaxation times with the experiments, like NMR, 2D-IR, and time dependent fluorescence Stokes shift. We discuss how these different experiments preferentially probe different aspects of this distribution and can thus lead to different results, leading to certain unnecessary confusion and controversy.

The organization of the rest of the paper is as follows. First, we try to show how the PHL is different from a bulk solvent with respect to (i) first and second rank orientational correlation time constants (τ_1 and τ_2) of the hydration layer water molecules which account for rotational diffusion and (ii) "translation time" distribution of water molecules in the PHL and quantification using the Heaviside step function formalism that accounts for the translational diffusion. Second, we calculate two equilibrium properties of the successive hydration layers, namely, effective dielectric constant (ε_{eff}) and specific heat (C_v^{eff}) in comparison to that of bulk water. Third, we show how the dynamics of solvation of a spherical virtual probe changes as it resides at various sites inside the PHL. The conclusions are drawn based on these results obtained for four protein-water systems, namely, the antimicrobial protein *lysozyme* (PDB ID: 1AKI), oxygen storage and transport protein *myoglobin* (PDB ID: 3E5O), immunoglobulin binding *protein-G* (PDB ID: 2GB1), and sweet protein *monellin* (PDB ID: 2O9U) in order to distinctly characterise and draw general remarks on the hydration layer and its uniqueness. The four proteins are chosen because of their diverse structure, function, and helix-sheet ratio (see Fig. 1 for details).

II. SYSTEM AND SIMULATION DETAILS

Atomistic molecular dynamics simulations are performed using the GROMACS[46] package (v5.0.7). We have prepared the system in accordance with experimental concentration (~2-3 mM). Initial configurations of the proteins have been taken from crystal structures available in the Protein Data Bank. We have used the Optimized Potentials for Liquid Simulations - All Atom (OPLS-AA) force field[48] and extended point charge (SPC/E) water model. Periodic boundary conditions were implemented using cubic boxes of sides ~9-10 nm filled with ~23 000-26 000 water molecules depending on the size of the protein. The total system was energy minimised using the steepest descent algorithm followed by the conjugate gradient method. Thereafter the system was subjected to simulated annealing[49] in order to heat it up from 300 K to 320 K and again cool it down to 300 K in order to unbias the system and help it to get out of a local minima (if any). The solvent was equilibrated for 10 ns at constant temperature (300 K) and pressure (1 bar) (NPT) by restraining the positions of the protein atoms followed by NPT equilibration for another 10 ns without position restrain. The final production runs were carried out at a constant temperature (T = 300 K) (NVT) for 30 ns. Analyses were performed on the last 25 ns of the trajectories to get rid of effects of a barostat. The equations of motions were integrated using the leap-frog integrator with an MD time step of 1 fs. All

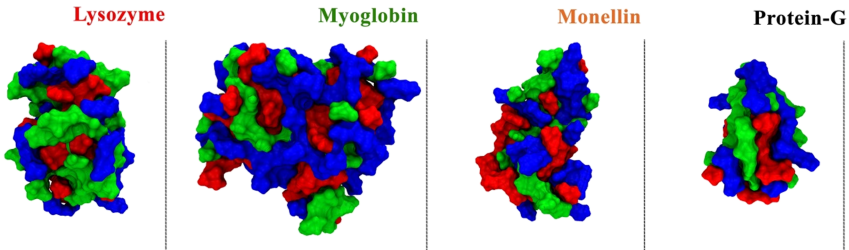

	Lysozyme	Myoglobin	Monellin	Protein-G
Volume(nm^3)	22±2	27±1	19±3	11±2
% helix	43	81	17	25
% strand	9	0	48	41
SASA(nm^2)	69±1	88±3	68±2	39±1
% hydrophilic SASA	55	48	50	57
Total dipole moment (D)	165	216	227	159

FIG. 1. Surface representations of four model protein systems along with some crucial parameters. Hydrophobic residues are shown in red, polar and uncharged residues are shown in green, and charged residues are in blue. The percentage of different secondary structures is obtained using the Stride package.[45] Average volume and SASA have been calculated using Gromacs[46] from 20 ns trajectories. The figures have been prepared using VMD.[47]

reported data are averaged over three MD trajectories starting from an entirely different configuration of the system. We have used the modified Berendsen thermostat[50] ($\tau_T = 0.1$ ps) and the Parrinello-Rahman barostat[51] ($\tau_P = 2.0$ ps) to keep the temperature and pressure constant, respectively. The cutoff radius for neighbour searching and non-bonded interactions was taken to be 10 Å, and all the bonds were constrained using the LINCS[52] algorithm. For the calculation of electrostatic interactions, the Particle Mesh Ewald (PME)[53] method was used with a FFT grid spacing of 1.6 Å.

III. RESULTS AND DISCUSSIONS

A. Distribution of rotational time constants

One of the most interesting and somewhat unexpected outcomes of the present study is the observation of a broad distribution of relevant relaxation times obtained from rotational relaxation and translational diffusion of water molecules. In Figs. 2 and 3, we show such distribution of relaxation times obtained for time correlation functions of several different dynamical quantities. Note the completely different nature of distribution compared to that of the bulk.

In order to characterise the distinctiveness in terms of rotation of one O–H bond of water molecules, we calculate the first and second rank orientational correlation [Eqs. (1) and (2)] for those water molecules which reside more than 100 ps inside the hydration layer and are monitored till they leave the PHL in order to obtain a good statistical averaging. We define a particular water molecule inside the hydration layer only when it is within 1 nm of its nearest protein atom. For the bulk solvent, the distribution is calculated for ~4000 water molecules averaged over a 10 ns trajectory,

$$C_1(t) = \langle P_1(\hat{\mu}_0.\hat{\mu}_t)\rangle, \quad \text{where } P_1(x) = x, \tag{1}$$

$$C_2(t) = \langle \mathrm{P}_2(\hat{\mu}_0.\hat{\mu}_t)\rangle, \quad \text{where } \mathrm{P}_2(x) = \tfrac{1}{2}(3x^2 - 1). \tag{2}$$

Here, P_1 and P_2 are, respectively, the first and second rank Legendre polynomials and μ_t are the unit vectors along any one O–H bond vector at time "t." The thus obtained rotational time correlation functions for each individual water molecules are fitted to a multi-exponential function and the time constants are obtained by integrating the area under each curve. The distributions (histogram) of those time constants are also broad and log-normal in nature, with a long tail extending up to a few hundred ps (Figs. 2 and 3). The averaged time correlation functions (i.e., averaged over all the water molecules considered) for each of the proteins are shown in Figs. 2 and 3 (inset) and the fitting parameters are noted down in Tables I and II.

Figures 2 and 3 depict that the distributions in protein hydration layers are broad and it is a trademark of dynamic heterogeneity. More interestingly, there are few water molecules (~4%-5% but varies from protein to protein) that relax faster than bulk water molecules along with a large fraction of slowly rotating water molecules. The faster rotating water molecules inside the hydration layer are proved to be those which are hydrogen bonded to a protein backbone.[54] *The average rotational retardation factors are ~2.5-3.0 as compared to the bulk*. This retardation factor has also been observed by NMR[29] and recent 2D-IR experiments.[55] If we look at the components of the relaxation, there is an extra time scale of amplitude ~18%-25% in the range of ~38-42 ps for lysozyme, myoglobin, and protein-G and ~28 ps for monellin which is absent in the case of bulk relaxation. The extra slow component arises presumably due to the long lived and strong hydrogen bonds that water forms with the charged residues (like Arg, Lys, Asp, etc.) on the protein surface. Because of this kind of broad distribution, the PHL always shows heterogeneous dynamical responses. On the other hand, experimental techniques like NMR or 2D-IR are sensitive towards slow and ultrafast dynamics, respectively. Moreover they provide only the average picture and not the microscopic details. Though this kind of detailed distributions cannot be obtained experimentally, the MRD technique claims to be successful at measuring the width of the distribution.[29] The broad spectrum of rotational relaxation pattern is responsible for the heterogeneous solvation dynamics throughout the PHL.[33,56]

B. Distribution of total dipole moment of hydration layer

Apart from the widely variant dynamical features of the hydration layer and bulk water discussed in Sec. III A, some thermodynamic response functions are also quite efficient in discriminating between PHL and bulk. One of such properties is the effective dielectric constant of the shell which is a response function of total dipole moment fluctuation. The magnitude of total dipole moment (M_T) of a particular domain is given by the following equation:

$$M_T = \sqrt{\sum_j \left(\sum_{i=1}^{N} \mu_j^i\right)^2}. \tag{3}$$

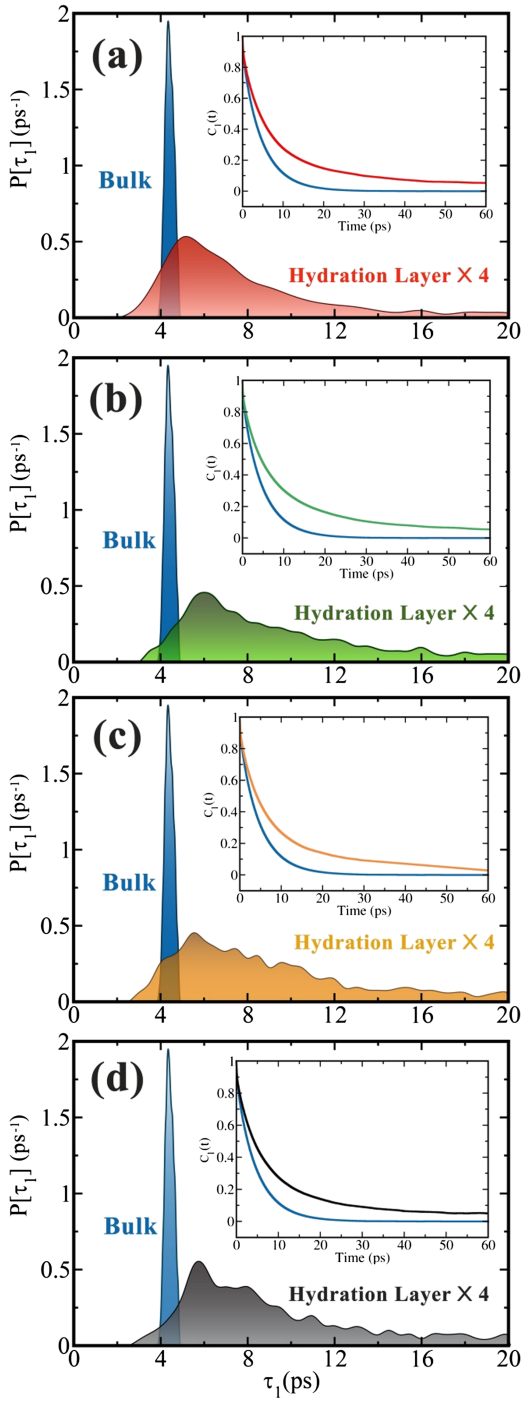

FIG. 2. Distribution of first rank rotational constants of water molecules inside the protein hydration layer for four proteins and bulk (blue). In the insets, the normalised and averaged rotational time correlation function is shown using same colour codes. (a) Lysozyme, (b) myoglobin, (c) monellin, and (d) protein-G.

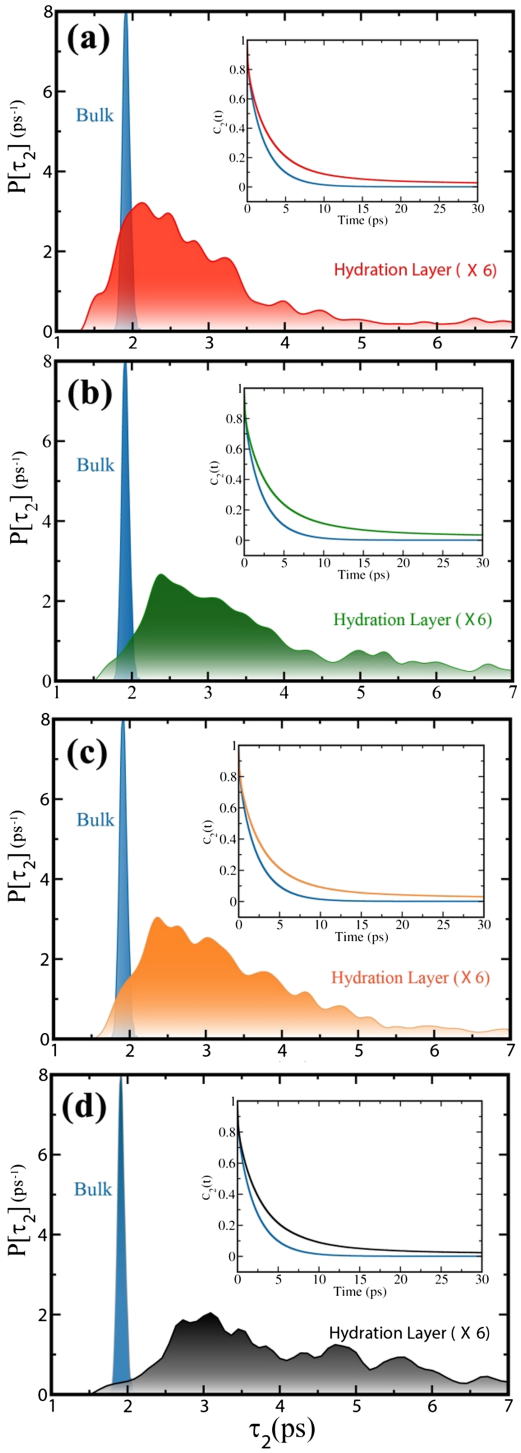

FIG. 3. Distribution of second rank rotational constants of water molecules inside the protein hydration layer for four proteins and bulk (blue). In the insets, the normalised and averaged rotational time correlation function is shown using the same colour codes. (a) Lysozyme, (b) myoglobin, (c) monellin, and (d) protein-G.

Here, "*i*" is the running index denoting water molecules and "*j*" is the index for Cartesian vector components (x,y,z) of dipole moment. This reflects a collective orientation of the water molecules. In the presence of a huge and constant dipole moment arising from protein (see Fig. 1), these orientations of water molecules are tremendously perturbed as compared to the bulk, causing significant reduction in the fluctuation of total dipole moment of that region.

Figure 4 supports the foregoing discussion. It shows the distributions of total dipole moment fluctuation of the first hydration layer of four proteins compared to that of the bulk. Because of the decrease in fluctuation of total dipole moment in the hydration layer as discussed above, a considerable narrowing of the distribution is observed. This distribution of the bulk is obtained by constructing an analogous shell in

TABLE I. Multi-exponential fitting parameters of the averaged and normalised first rank rotational relaxation of hydration layer water molecules and that of the bulk. The slowest of the time scales (noted down in bold) was absent in the bulk solvent.

	a_1	τ_1 (ps)	a_2	τ_2 (ps)	a_3	τ_3 (ps)	$\langle\tau\rangle$ (ps)	Average retardation
Lysozyme	0.13	0.21	0.66	5.63	**0.21**	**38.6**	11.85	2.76
Myoglobin	0.16	0.34	0.63	6.38	**0.21**	**40.3**	12.53	2.92
Protein-G	0.14	0.29	0.68	6.14	**0.18**	**41.4**	11.66	2.72
Monellin	0.11	0.15	0.63	5.06	**0.26**	**28.1**	10.51	2.45
Bulk water	0.13	0.21	0.87	4.93	...	...	4.29	1.00

bulk water maintaining the same volume and shape of the PHL.

For this narrow distribution inside the PHL, the dielectric constant becomes lower than that of the bulk, as also observed by Ghosh *et al.*[42] We calculate this property using the well-known expression in terms of total dipole moment fluctuation[57–59] as shown in the following equation:

$$\varepsilon = 1 + \frac{4\pi}{3Vk_BT}\left\langle (M_T - \langle M_T\rangle)^2\right\rangle. \tag{4}$$

An important point to be noted in this context is that the definition of an "*effective dielectric constant*" of the hydration layer is valid only in the limiting condition that the cross correlation coefficient [Eq. (10)] between total dipole moment fluctuations of PHL and the same of the next layer should be low (~10% or so). An analytical description of the issue is given below. Considering the total dipole moment of water to be $\overline{M}_W$, we can write

$$\left\langle \delta\overline{M}_W^2\right\rangle = \left\langle \sum_i \delta\overline{M}_W^{i\,2}\right\rangle + 2\left\langle \sum_i \sum_{j\neq i} \delta\overline{M}_W^i \delta\overline{M}_W^j\right\rangle, \tag{5}$$

where i and j are indices denoting the shell around the protein. Hence the total dipole moment of water has one self-part and a cross-part. Now, if the cross term is negligible, we can rewrite Eq. (5) as

$$\left\langle \delta\overline{M}_W^2\right\rangle = \left\langle \sum_i \delta\overline{M}_W^{i\,2}\right\rangle = \sum_i \left\langle \delta\overline{M}_W^{i\,2}\right\rangle. \tag{6}$$

Scaling Eq. (6) with respect to volume, we obtain

$$\frac{\left\langle \delta\overline{M}_W^2\right\rangle}{V_W} = \sum_i \frac{\left\langle \delta\overline{M}_W^{i\,2}\right\rangle}{V_W} = \sum_i \left(\frac{\left\langle \delta\overline{M}_W^{i\,2}\right\rangle}{V_W^i}\right)\times\left(\frac{V_W^i}{V_W}\right), \tag{7}$$

TABLE II. Multi-exponential fitting parameters of the averaged and normalised second rank rotational relaxation of hydration layer water molecules. The slowest of the time scales (noted down in bold) was absent in the bulk solvent.

	a_1	τ_1 (ps)	a_2	τ_2 (ps)	a_3	τ_3 (ps)	$\langle\tau\rangle$ (ps)	Average retardation
Lysozyme	0.23	0.16	0.70	3.17	**0.07**	**33.67**	4.59	2.43
Myoglobin	0.25	0.18	0.67	3.55	**0.08**	**37.56**	5.81	3.07
Monellin	0.21	0.11	0.68	2.93	**0.11**	**21.70**	4.40	2.33
Protein-G	0.24	0.17	0.70	3.40	**0.06**	**35.39**	4.54	2.40
Bulk water	0.22	0.13	0.78	2.39	...	...	1.89	1.00

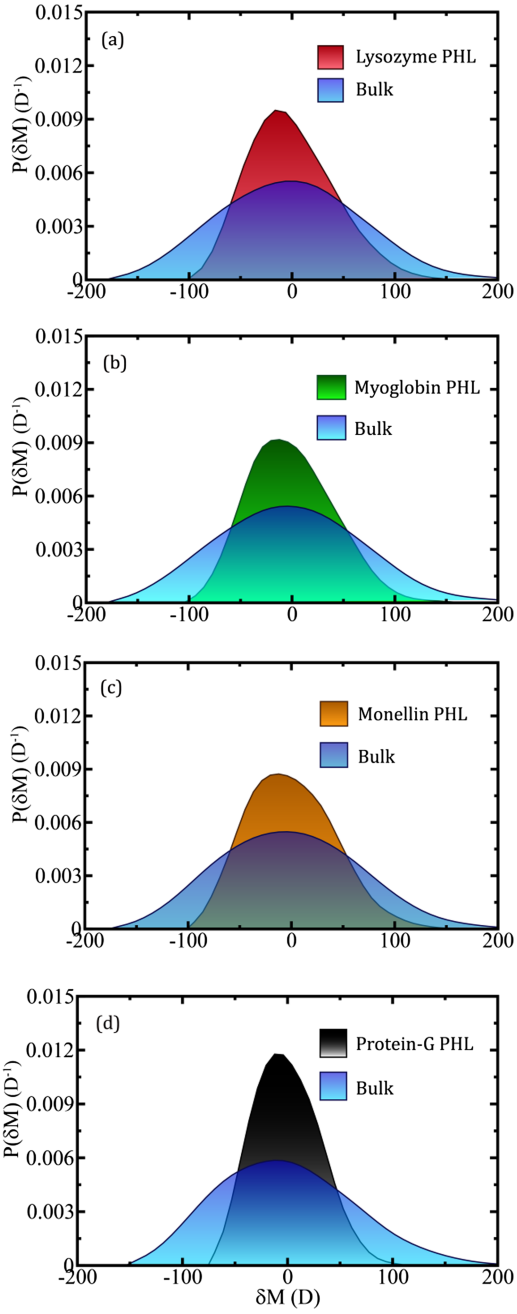

FIG. 4. Comparison of distributions of total dipole moment fluctuations (in debye unit) in the first hydration layer of four proteins and that of the bulk (blue). (a) Lysozyme (red), (b) myoglobin (green), (c) monellin (orange), and (d) protein-G (black). The width of distribution in the case of the hydration layer becomes almost half as compared to the bulk.

where V_W is the volume of the total water and V_W^i is the volume of the ith water shell. Multiplying both sides of Eq. (7) with the factor $\frac{4\pi}{3k_BT}$ and defining volume fraction of ith shell as $v_f^i = \frac{V_W^i}{V_W}$, we get

$$\frac{4\pi\left\langle \delta\overline{M}_W^2\right\rangle}{3V_Wk_BT} = \frac{4\pi}{3k_BT}\sum_i \left(\frac{\left\langle \delta\overline{M}_W^{i\,2}\right\rangle}{V_W^i}\right)v_f^i,$$
$$\text{hence,}\quad \varepsilon_W = \sum_i v_f^i\varepsilon_i, \tag{8}$$

where ε_W is the dielectric constant for all the water molecules in the system and ε_i is the effective dielectric constant of the

ith hydration shell, which is defined by the following equation:

$$\varepsilon_i^{eff} = 1 + \frac{4\pi}{3V_W^i k_B T}\left\langle \left(M_W^i - \left\langle M_W^i \right\rangle\right)^2 \right\rangle. \quad (9)$$

The measure of smallness of the cross terms with respect to the self-terms is defined using the well-known expression of correlation coefficient (ρ_{12}) as shown in the following equation:

$$\rho_{12} = \frac{\mathrm{cov}(M_1, M_2)}{\sqrt{\mathrm{var}(M_1)\,\mathrm{var}(M_2)}} = \frac{\langle (M_1 - \langle M_1\rangle)(M_2 - \langle M_2\rangle)\rangle}{\sqrt{\left\langle (M_1 - \langle M_1\rangle)^2\right\rangle \left\langle (M_2 - \langle M_2\rangle)^2\right\rangle}}. \quad (10)$$

Here, angular brackets denote average over time. M_1 and M_2 are the total dipole moment of first and second layers, respectively. The protein surface is generally rugged even for a globular protein (Fig. 5). The width of the PHL and second layer is judicially chosen to be 1 nm and 2 nm, respectively, to avoid the effect of protein surface heterogeneity so that the cross correlation becomes negligible across the layers and there is not much discrepancy in the volume calculation in case we consider the shell to be spherical (Table III). To get the volume of the hydration layer, we have used the specific volume of water at 300 K along with the number density calculated from our MD trajectories.

We also calculate the total moment-moment autocorrelation function and compare it with the same in the bulk. The autocorrelation relaxations are fitted bi-exponential forms for PHL and single-exponential form for the bulk water. There is always a slower component of one order of magnitude higher in the case of the PHL compared to the bulk.[42] The relaxation is generally slower because of the large dipole moment of the protein which itself prevents the surrounding water dipoles to relax rapidly. For the beta sheet rich proteins GB1 and monellin, the average retardation factor is ∼1.5 and for that of alpha helix rich proteins lysozyme and myoglobin, it is ∼2.5. The fitting parameters are summarized in Table IV and the plots are shown in Fig. 6.

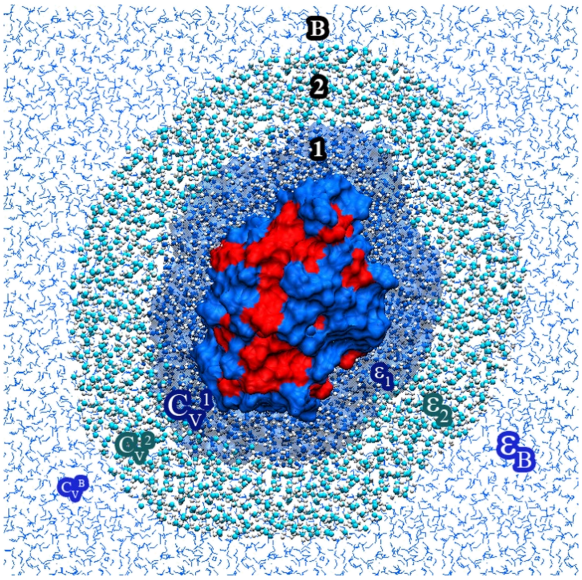

FIG. 5. Protein surrounded by water layers (cross section); layer-1 is the PHL. Effective dielectric constant of water shell increases and local specific heat decreases as we move away from protein, i.e., $\varepsilon_1 < \varepsilon_2 < \varepsilon_{Bulk}$, whereas $C_V{}^1 > C_V{}^2 > C_V{}^{Bulk}$.

TABLE III. Effective dielectric constants of the protein hydration layer, second layer, and bulk water in the case of four protein water systems. The cross correlation coefficients are also tabulated and found to be ∼10% compared to self-term. Indices "1," "2," and "B" signify PHL, shell-2, and bulk, respectively.

	Lysozyme	Myoglobin	Monellin	Protein-G
ε^{eff} (shell-1)	46.54	44.39	48.67	43.24
ε^{eff} (shell-2)	54.01	52.38	63.25	55.96
ε (bulk)		68.77		
ρ_{12}	0.15	0.09	0.12	0.14

C. Distribution of water self-interaction energy of hydration layer

Besides dipole moment, total self-interaction energy (Coulomb and Lennard-Jones (LJ)) distribution of PHL and bulk water molecules is also widely different. For the bulk, it is sharp and narrow, whereas in the case of the PHL, it is generally wider (Fig. 7). For the bulk, the FWHM (Full Width at Half Maximum) is ∼400 k_BT, whereas the same for lysozyme, myoglobin, monellin, and protein-G is ∼1060, ∼860, ∼690, and ∼1030 k_BT, respectively.

Energy fluctuation is manifested in the form of the static response function specific heat[31] (C_V) given by the following equation:

$$C_V = \frac{1}{k_B T^2}\left\langle (E - \langle E\rangle)^2 \right\rangle. \quad (11)$$

This energy fluctuation can have two contributions arising from potential energy and kinetic energy. For the PHL, the potential or interaction energy term has two parts: one self-term and the other cross term. Hence variance of potential energy for the PHL can be expressed using the following equation:

$$\left\langle \left(\delta E^1\right)^2 \right\rangle = \left\langle \left(\sum_i \delta E_i\right)^2 \right\rangle + \left\langle \left(\sum_{i,j} \delta E_{i,j}\right)^2 \right\rangle + 2\left\langle \left(\sum_i \delta E_i\right)\left(\sum_{i,j} \delta E_{i,j}\right) \right\rangle. \quad (12)$$

TABLE IV. Multi-exponential fitting parameters for ⟨δM(0)δM(t)⟩ of the PHL and bulk solvent. There exist a slower component in the case of the PHL which is absent in the bulk.

	a_1	τ_1 (ps)	a_2	τ_2 (ps)	⟨τ⟩ (ps)	Average retardation
Lysozyme	0.86	9.26	0.14	132.2	26.47	2.69
Myoglobin	0.85	8.64	0.15	120.05	25.35	2.58
Monellin	0.91	9.35	0.09	72.59	15.04	1.53
Protein-G	0.90	9.07	0.10	81.87	16.35	1.66
Bulk solvent	1.00	9.81	...	...	9.81	1.00

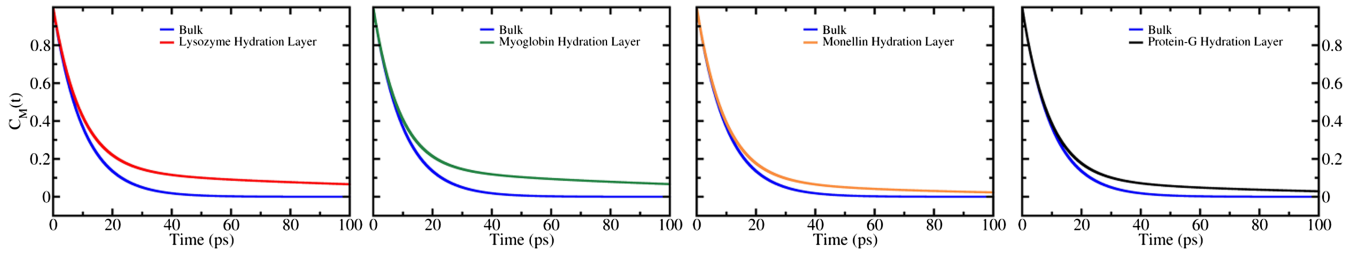

FIG. 6. Plots of total moment-moment autocorrelation function for the protein hydration layer and bulk. The same as that of the bulk solvent is shown in blue and for the proteins pervious colour codes are retained. Lysozyme (red), myoglobin (green), monellin (orange), and protein-G (black).

$\sum_i \delta E_i$ is the self-interaction energy among water molecules in the PHL, whereas $\sum_{i,j} \delta E_{i,j}$ is the cross interaction energy between molecules in the PHL and rest of the system. Hence in the limiting condition that self-interaction is much greater than cross-interaction, we have

$$\lim_{\frac{\sum_{i,j} \delta E_{i,j}}{\sum_i \delta E_i} \to 0} \left\langle \left(\delta E^1\right)^2 \right\rangle = \left\langle \left(\sum_i \delta E_i\right)^2 \right\rangle. \quad (13)$$

This allows us to define a local specific heat of the PHL having self-energy contribution only, following the definition in Eq. (11).

We may derive specific heat like quantity for kinetic energy contribution as well, since this includes the individual molecules themselves. These results are tabulated in Table V. It is observed that the specific heat values of the PHL are more than twice of that of bulk values for both potential and kinetic energy contributions. The sum of the two gives the total effective heat capacity of different shells around the protein. In all the cases, specific heat is found to be greater than twice that of bulk water.

A greater value of specific heat points towards a greater fluctuation in energy. Analogous to the case of dipole moment, energy of an aqueous system is also highly perturbed by the presence of a large biomolecule like protein. The side chains of protein residues undergo continuous ceaseless conformational fluctuations which generate random kicks on the nearby water molecules. This results in an increased energy fluctuation in the hydration layer water molecules. Consequently, the specific heat of the layer also increases.

This increased specific heat is an indication of increased resistance towards the temperature change of water molecules inside the PHL because in the NVT ensemble, the specific heat at constant volume is proportional to the energy fluctuation [Eq. (11)]. So it would be twice or thrice as difficult to change the local temperature of the PHL as it is in the bulk. As the function of a particular protein is sensitive to the local temperature of the surroundings, the PHL plays a huge role to provide that environment acting like a shield.

D. Translation time of water molecules inside hydration layer

We first define the residence time of a single water molecule as the time spent inside the ~1 nm shell (chosen as the width of the hydration layer) from the surface of a protein. We also compare it with the residence time of bulk water by concentrating on a similar sized shell which equals the PHL in volume, but without having the protein inside. We find that the *mean residence time* is within ~90-100 ps when the protein is present but reduces to only ~30-40 ps in the absence of the protein. From there, we calculate the time required for a water

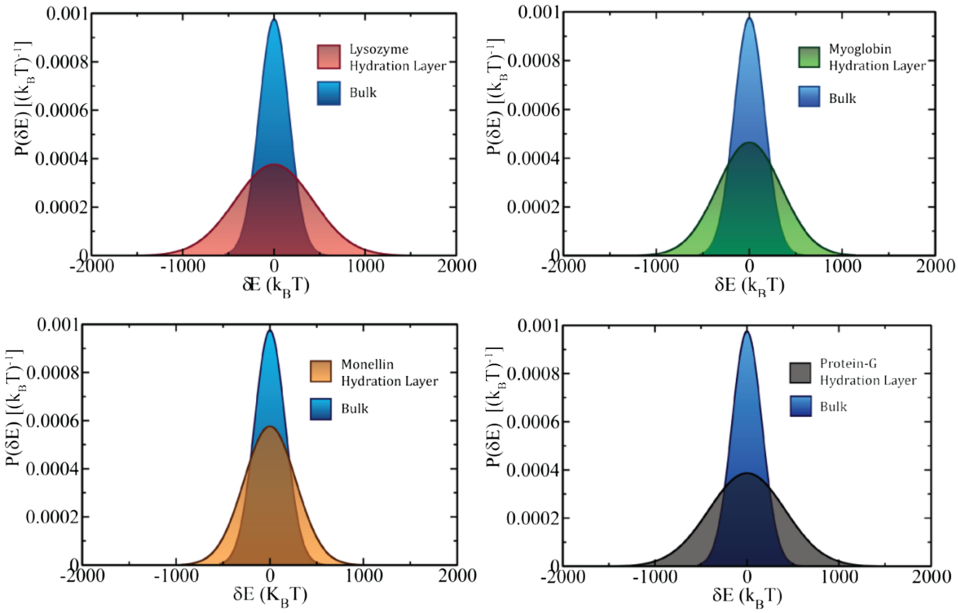

FIG. 7. Distribution of total self-interaction energy of the protein hydration layer compared with the bulk (blue). For every protein-water system, the distribution is broader than the bulk. This implies a larger specific heat of the hydration layer sub-ensemble as in the NVT ensemble the width of the distribution is proportional to the specific heat at constant volume.

TABLE V. Effective specific heat of PHL and shell-2 of four proteins compared to that of the bulk. The table contains data for both potential and kinetic energy contributions. C_V values are in cal K^{-1} g^{-1} unit.

Contribution	Shell#	Lysozyme	Myoglobin	Monellin	Protein-G	Bulk
Potential energy	1	1.89	1.79	1.69	1.74	0.74
	2	1.63	1.34	1.03	1.58	
Kinetic energy	1	0.62	0.75	0.65	0.56	0.32
	2	0.77	0.90	0.45	0.71	
Effective specific heat	1	2.51	2.54	2.34	2.30	1.06
	2	2.40	2.24	1.48	2.29	

molecule residing inside the PHL to translate by the same distance as its LJ diameter (σ = 0.316 nm for the SPC/E water model). We find that in the bulk solvent this value averaged around 3.3 ps, but in the case of the PHL we again see a broad distribution varying from protein to protein. All of the distributions have a distinct long tail extending up to ~30 ps–40 ps. The distributions are given in Fig. 8.

There are water molecules which translate faster than the molecules in the bulk along with the slower and bulk like ones. If we choose the average value of the sharp bulk distribution as the boundary to call a water molecule "fast" or "slow," we end up with the following numbers tabulated in Table VI. The faster translating ones are near hydrophobic regions facing a repulsive potential. The faster movement also arises from the "kicking motion" produced by long and extended amino acid side-chains such as arginine and lysine. Because of the low rotational barrier,[60] incessant side-chain conformation fluctuations introduce a constant perturbation to the hydration layer which in turn increases the energy content of the same. This is manifested in the high specific heat of the hydration layer (see Sec. III B).

In order to quantify the obtained residence times with the help of a suitable time correlation function, we define s(t) [see Eq. (14)], which is a measure of the lifetime of a water molecule inside the hydration layer. It is defined as

$$s(t) = \frac{\langle h(0)h(t)\rangle}{\langle h(0)h(0)\rangle}. \tag{14}$$

Here, "h(t)" is a *Heaviside step function*[61] at time "*t*" that describes the "in-or-out" state of a water molecule. It takes up a value of "1" when the water molecule is inside the PHL and "0" otherwise. In addition to that we use an "*overlook period*" of 2 ps (which is small compared to the mean residence time inside the PHL). If a particular water molecule, located at the imaginary boundary of the first shell and second shell, leaves the PHL for a duration which is less than the overlook period, we consider that to be continuously inside the PHL. Once it is outside the PHL for more than 2 ps, we consider that to be a "0" state from that time forever. This allows us to treat those water molecules which cannot get stabilised outside the PHL and comes back again to the first shell. We calculate s(t) for each individual water molecules inside the PHL and take an average over the molecules. The resultant time correlation functions are fitted to a multi-exponential (Table VII, Fig. 9) and by integrating over time we extract the mean lifetime of water molecules inside the PHL.

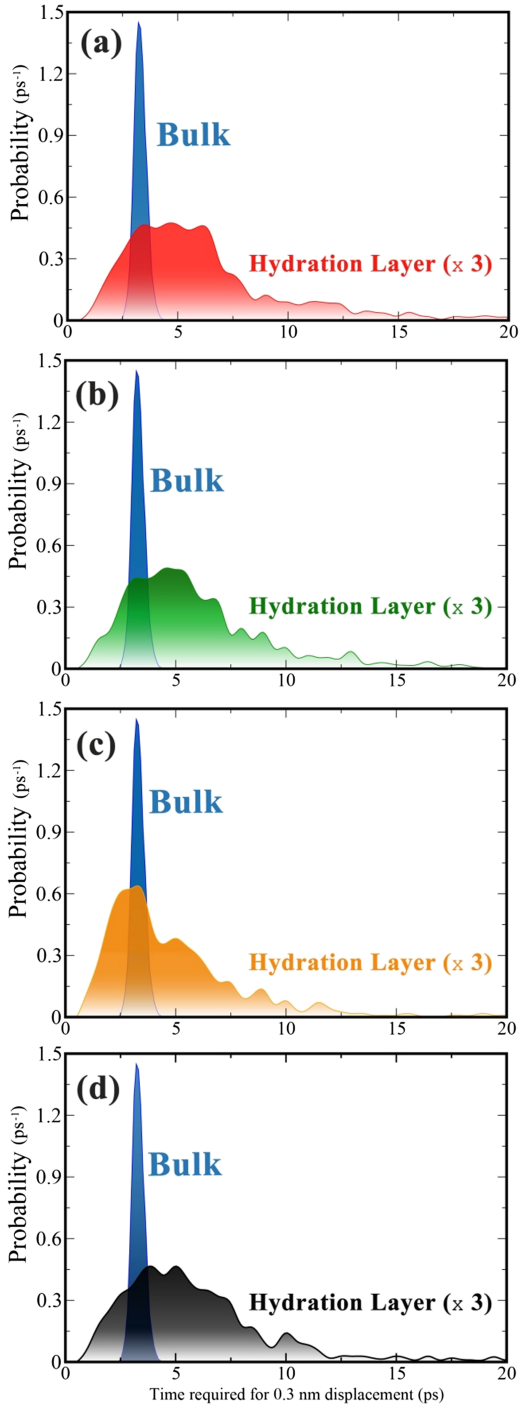

FIG. 8. Broad distribution of the time required to get displaced equal to one molecular diameter for water molecules in the bulk (shown in blue) and inside protein hydration layer ranging from 1 ps to 20 ps for (a) lysozyme (red), (b) myoglobin (green), (c) monellin (orange), and (d) protein-G (black). Noticeably there exist some water molecules which travel faster than the bulk.

From Table VII it is clear that the average retardations (defined as $\langle\tau\rangle_{hyd}/\langle\tau\rangle_{bulk}$) are ~2.3-2.6 compared to the bulk. But the measure cannot promulgate the existing broad distribution which is the primary reason for the uniqueness of PHL. Moreover, there exists one such time scale which is of one order of magnitude higher than that of the bulk. But again the average value cannot capture this. Due to the presence of this heterogeneity, the unique properties of PHL arise along with the site dependant local responses.

TABLE VI. Fraction of fast and slow translating water molecules inside the protein hydration layer of four different protein-water systems.

	% of translationally fast water	% of translationally slow water	Average time taken to translate by σ(ps)	Average retardation compared to the bulk
Lysozyme	23	77	6.9	2.09
Myoglobin	18	82	6.6	2.00
Monellin	35	65	5.3	1.61
Protein-G	27	73	6.0	1.82
Bulk water	...	...	3.3	1.00

TABLE VII. Multi-exponential fitting parameters of the normalised residence time correlation function, s(t), using the Heaviside step function formalism for hydration layer water molecules and for bulk water. (The timescales that are greater than one order of magnitude than that of the bulk are highlighted using boldface type.)

	a_1	τ_1 (ps)	a_2	τ_2 (ps)	a_3	τ_3 (ps)	$\langle\tau\rangle$ (ps)	Average retardation
Lysozyme	0.29	9.2	0.47	74.5	0.24	**244.3**	96.32	2.46
Myoglobin	0.25	7.5	0.41	58.8	0.34	**219.6**	100.6	2.57
Monellin	0.24	5.2	0.45	53.1	0.31	**213.6**	91.36	2.33
Protein-G	0.21	5.9	0.41	47.2	0.38	**185.6**	91.12	2.32
Bulk water	0.17	3.4	0.36	21.4	0.47	65.7	39.16	1.00

E. Heterogeneous solvation dynamics inside hydration layer

Because of the multitude of rotational and translational time scales inside the PHL, the dynamics of solvation becomes a site dependent phenomenon throughout the hydration layer. In Sec. III A, we have shown that there are a few water molecules that are rotating faster than bulk water molecules although the majority of water molecules in the hydration layer are slower. In order to explore this aspect, we put virtual probes at different sites of the PHL. A virtual probe is a spherical point positive charge with 0.5 Å radius which is fixed with respect to an atom on the protein surface. We have used four spheres situated at different locations inside the PHL for each protein to probe the dynamical response of different sites. The interaction energies are taken to be the sum of Coulomb and LJ interactions.[62] Linear response theory[63] is applied on each energy trajectory to find out the solvation time correlation function[62,64–67] [Eq. (15)] and the time scales are obtained using a multi-exponential fitting equation with a Gaussian component to take care of the initial sub ~100 fs ultrafast decay[68] (see Table VIII for details),

$$C(t) = \frac{\langle \delta E_{solv}(0)\delta E_{solv}(t)\rangle_{gr}}{\langle \delta E_{solv}(0)^2\rangle_{gr}}. \quad (15)$$

Here, $\delta E_{solv}(t)$ is the fluctuation given by $\delta E_{solv}(t) = E_{solv}(t) - \langle E\rangle$. The subscript "$gr$" indicates the averaging over ground state only.[41]

The time constant of solvation of a bare ion in water is extremely fast.[64,65] This can be partly (not fully) realised with the help of the following equation:

$$\tau_L = \left(\frac{\varepsilon_\infty}{\varepsilon_0}\right)\tau_D. \quad (16)$$

Debye relaxation time τ_D is 8.3 ps for water. ε_∞ and ε_0 are the infinite frequency and static dielectric constants for water. ε_0 is ~78 and ε_∞ is ~5. Solvation energy relaxation time for an ion would then be 500 fs is water. Now the value for ε_0 decreases as we move closer towards the protein surface.[42] This results in a slower solvation. But there are other governing factors as well, such as the inertial component and the heterogeneity of time scales. Because of the broad distributions of dynamical quantities inside the PHL, different sites measure responses in a different manner when it comes to a partly local probe like solvation.

As expected, different locations show different time scales of solvation (Fig. 10) though the average time constants are close to each other. As pointed out in earlier studies, solvation becomes slow near charged side-chains, not only due to slow water molecules but also because of the contribution of the charged/polar amino acid side chains.[33] The regions which contain fast rotating water molecules generally have a faster solvation. These regions are near the backbone of protein and near hydrophobic groups.

However, as in the case of NMR, TDFSS also suffers from being able to measure only an average property except that one can use the location of the probe to get more insight into the distribution of relaxation times.

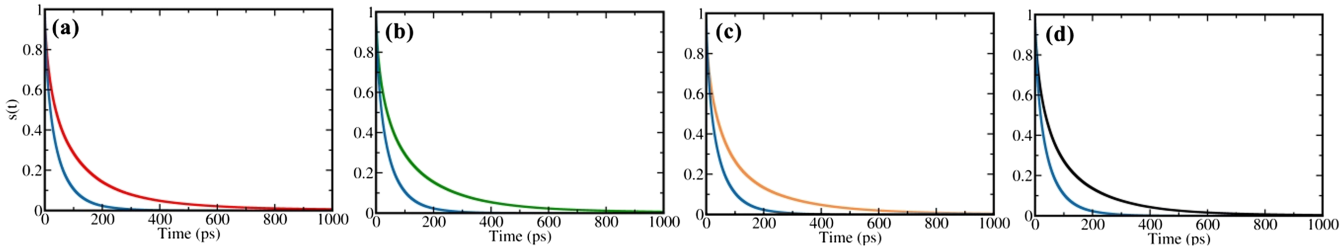

FIG. 9. Residence time correlation using the Heaviside step function formalism of PHL compared with the same in bulk water (blue). (a) Lysozyme (red), (b) myoglobin (green), (c) monellin (orange), and (d) protein-G (black). The average time constant shows a ~2.5 times slowdown for PHL water molecules.

TABLE VIII. Multi-exponential fitting parameters for the solvation correlation function of virtual probes situated at different positions inside the protein hydration layer. The probe is placed within ∼2-3 Å from a particular residue. The parameters are obtained after fitting the obtained normalised correlation to $C(t) = a_g e^{-(t/\tau_g)^2} + \sum_{i=1}^{n} a_i e^{-(t/\tau_i)}$.

Protein	Probe location	a_g, τ_g (ps)	a_1, τ_1 (ps)	a_2, τ_2 (ps)	$\langle\tau\rangle$ (ps)
Lysozyme	Near Trp-123	0.61, 0.077	0.25, 0.66	0.14, 9.42	1.53
	Near Trp-63	0.69, 0.074	0.23, 0.61	0.08, 12.22	1.16
	Near Trp-111	0.63, 0.095	0.28, 3.85	0.09, 107.53	10.81
	Near Trp-28	0.69, 0.089	0.23, 2.42	0.08, 50.24	4.63
Myoglobin	Near Tyr-146	0.64, 0.073	0.24, 0.42	0.12, 7.39	1.03
	Near His-12	0.59, 0.079	0.25, 0.72	0.16, 7.42	1.41
	Near His-81	0.62, 0.074	0.27, 0.59	0.11, 10.02	1.30
	Near His-113	0.70, 0.072	0.24, 0.41	0.06, 10.59	0.78
Monellin	Near Tyr-62	0.65, 0.047	0.28, 0.76	0.07, 16.16	1.37
	Near Tyr-78	0.53, 0.048	0.31, 0.58	0.16, 7.74	1.44
	Near Tyr-46	0.55, 0.052	0.33, 0.65	0.12, 10.21	1.46
	Near Tyr-28	0.50, 0.050	0.35, 0.49	0.15, 8.24	1.43
Protein-G	Near Val-29	0.74, 0.079	0.19, 0.96	0.07, 20.89	1.69
	Near Tyr-33	0.68, 0.085	0.24, 1.48	0.08, 13.66	1.50
	Near Tyr-3	0.59, 0.078	0.27, 0.64	0.14, 8.44	1.39
	Near Val-54	0.73, 0.082	0.19, 1.11	0.08, 18.51	1.74

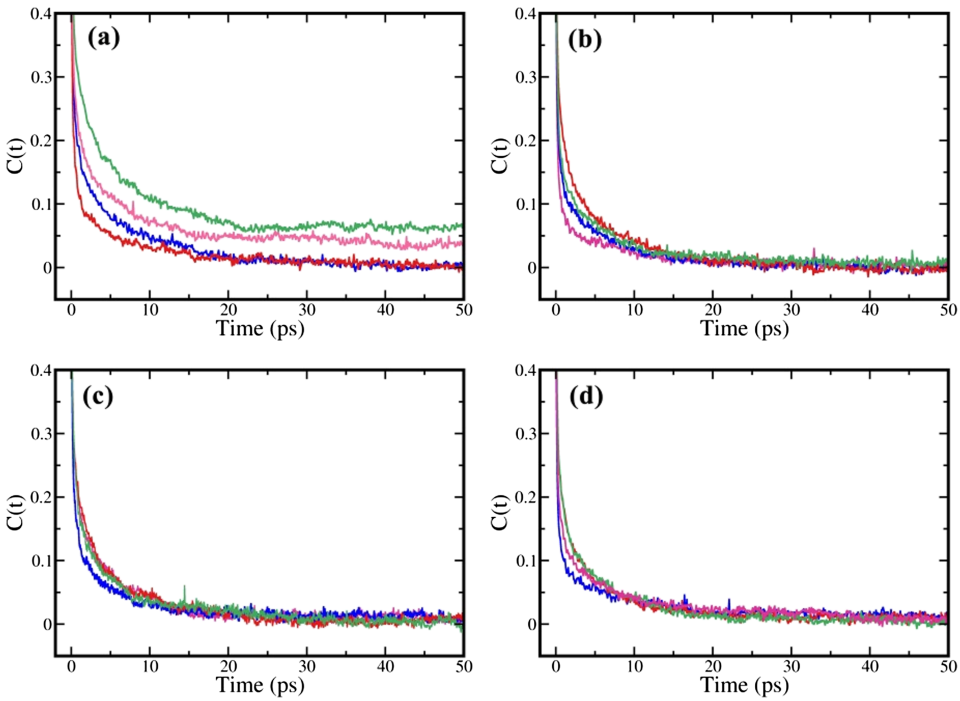

FIG. 10. Normalized total energy correlation plots for several virtual probes situated at different sites in the protein hydration layer of (a) lysozyme, (b) myoglobin, (c) monellin, and (d) protein-G. The plots are shown only from C(t) = 0.4 as the initial ∼60%-70% decay is ultrafast and ubiquitous. This difference in time scales shows the dynamical heterogeneity present inside the PHL.

IV. CONCLUSION

As discussed extensively in the context of single molecule spectroscopy,[69] the measured time correlation function is an ensemble averaged property. Just like we observed often in single molecule spectroscopy and also in supercooled liquids,[29,70] two different distributions can provide a similar time correlation function. It is thus possible to reach erroneous conclusions if we base them on the ensemble average properties alone. The average can be a poor measure of reality.

The main results of the present work can be summarized as follows. Distributions of calculated residence times and rotational relaxation times in the hydration layer for four different protein-water systems are unusually broad. The distributions are Gaussian in the bulk but transform to "log-normal" in the case of the hydration layer. Note that log-normality is

abundant in nature.[71] We can justify the deviation from Gaussian to log-normality by assuming that the relaxation times scale by a multiplicative factor of $e^{-\beta\Delta E_i}$ with respect to the bulk ($\Delta E_i = E_i^{PHL} - E_i^{Bulk}$, "$i$" is the water index). Inside the PHL, if a particular water molecule becomes more stable than that of the bulk, ΔE_i becomes negative. Hence, the factor takes up a positive value. As a result, elongation of relaxation times occurs. On the contrary, there exists a fraction of water molecules which becomes less stable in the PHL. For those, faster relaxation occurs (see the supplementary material for fits in Fig. 8).

Physically, this arises from the simultaneous presence of (a) peptide backbones that form weak hydrogen bonds, (b) hydrophobic amino acid side chains that form no hydrogen bond, and (c) charged polar groups that form a strong hydrogen bond with the surrounding water molecules. This broad distribution is not reflected in the average time constant which is just about 2-3 times larger than that of bulk water[29,34,55] (Tables IV and VI). In particular, the average leads to the erroneous conclusion that water in the hydration layer is bulk-like. Nevertheless, the mathematical description of log-normality is elusive and still deserves proper quantification.

The protein hydration layer is unique because the water molecules encounter a highly heterogeneous surface with respect to structure and electrostatics. The water molecules that are hydrogen bonded to the peptide back-bone are known to rotate and translate faster than those bonded to charge groups like arginine or glutamate or aspartate.[54] In addition, the solvent exposed hydrophobic amino acid side chains offer no specific resistance to the rotation of water molecules. Since different proteins could have substantially different sequence of amino acid residues, water dynamics could be quite sensitive to the specific nature of a particular protein. However, some aspects are conserved. As the peptide backbone should always be present, a part of relaxation of the hydration layer should always be faster than the bulk. The same goes for the water molecules near the hydrophobic residues. Therefore, one should be particularly concerned about the sensitivity to the charged amino acid groups. Only these groups can give rise to slower than the bulk decay. Experiments measure the ensemble averaged retardation factors which are obtained in our present study as well but cannot bring out the true characterisation.[29,55] The universal and defining characteristics of the hydration layer would then be a broad distribution of relaxation times, with relaxation times substantially shorter than the bulk to a range substantially higher than the bulk.

On top of that due to its low dielectric constant and high specific heat, it offers a unique property. Due to the low dielectric constant, the PHL cannot screen the interaction proteins do with ligands[72] (substrates, small molecules, drugs, etc.) which are the most important part before any protein action such as enzyme kinetics[73] or aggregations.[74,75] The high value of specific heat provides a protective environment around the protein which is more resistant to the temperature change that water molecules at the far. This helps the protein to function properly. We also discuss some aspects in favour of the uniqueness of the hydration layer. There are many other structural and dynamical properties [radial distribution, tetrahedral order parameter, dynamics structure factor, χ_4(t), etc.] that would serve equally good in this purpose. This can be extended to other biological macromolecules like DNA as well, given that their surface is heterogeneous.

The wide distribution of relaxation times could have the following important experimental ramifications. (i) The solvation dynamics could be highly non-exponential, as discussed. We have observed elsewhere that solvation dynamics can observe amino acid side chain motions and can be sensitive to slower than average dynamics.[1,12,32,33] One needs to untangle the observed dynamics to obtain water contribution. (ii) NMR experiments that isotope label peptide group atoms can preferentially probe the faster motions of, weakly hydrogen bonded water molecules,[28,29,76] (iii) 2D-IR experiments may also preferentially observe faster water molecules as these experiments also use isotope labelling of peptide group atoms.[29] Thus, results of both 2D-IR and NMR can be biased towards molecules exhibiting faster than average dynamics. Therefore, one needs to employ all the available techniques to understand and explore the wide distribution reported here, for the first time.

SUPPLEMENTARY MATERIAL

See supplementary material for brief descriptions of the algorithms used to obtain the distributions of relaxation times (Secs. S1 and S2). We also provide some exemplary plots to support our discussions. Apart from this, we include log-normal fitting parameters corresponding to distributions in Fig. 8 of Sec. S3.

ACKNOWLEDGMENTS

We are thankful to Dr. Rajib Biswas for many useful discussions and technical help. We thank the Department of Science and Technology (DST, India) for partial support of this work. B. Bagchi thanks Sir J. C. Bose fellowship for partial support. S. Mondal thanks UGC, India for providing research fellowship and S. Mukherjee thanks DST, India for providing INSPIRE fellowship.

[1] B. Bagchi, Proc. Natl. Acad. Sci. U. S. A. **113**(30), 8355–8357 (2016).
[2] D. Laage, T. Elsaesser, and J. T. Hynes, "Water dynamics in the hydration shells of biomolecules," Chem. Rev. (published online).
[3] H. Frauenfelder, G. Chen, J. Berendzen, P. W. Fenimore, H. Jansson, B. H. McMahon, I. R. Stroe, J. Swenson, and R. D. Young, Proc. Natl. Acad. Sci. U. S. A. **106**(13), 5129–5134 (2009).
[4] B. Bagchi, Chem. Rev. **105**(9), 3197–3219 (2005).
[5] D. Laage, G. Stirnemann, F. Sterpone, R. Rey, and J. T. Hynes, Annu. Rev. Phys. Chem. **62**, 395–416 (2011).
[6] P. Ball, "Water is an active matrix of life for cell and molecular biology," Proc. Natl. Acad. Sci. U. S. A. (published online).
[7] L. Zhang, L. Wang, Y.-T. Kao, W. Qiu, Y. Yang, O. Okobiah, and D. Zhong, Proc. Natl. Acad. Sci. U. S. A. **104**(47), 18461–18466 (2007).
[8] J. C. Rasaiah, S. Garde, and G. Hummer, Annu. Rev. Phys. Chem. **59**, 713–740 (2008).
[9] W. Qiu, Y.-T. Kao, L. Zhang, Y. Yang, L. Wang, W. E. Stites, D. Zhong, and A. H. Zewail, Proc. Natl. Acad. Sci. U. S. A. **103**(38), 13979–13984 (2006).
[10] W. Qiu, L. Zhang, O. Okobiah, Y. Yang, L. Wang, D. Zhong, and A. H. Zewail, J. Phys. Chem. B **110**(21), 10540–10549 (2006).
[11] B. Bagchi, *Water in Biological and Chemical Processes: From Structure and Dynamics to Function* (Cambridge University Press, 2013).
[12] D. Zhong, S. K. Pal, and A. H. Zewail, Chem. Phys. Lett. **503**(1), 1–11 (2011).

[13]S. M. Bhattacharyya, Z.-G. Wang, and A. H. Zewail, J. Phys. Chem. B **107**(47), 13218–13228 (2003).
[14]N. Nandi and B. Bagchi, J. Phys. Chem. B **101**(50), 10954–10961 (1997).
[15]R. Pethig, Annu. Rev. Phys. Chem. **43**(1), 177–205 (1992).
[16]E. Grant, Bioelectromagnetics **3**(1), 17–24 (1982).
[17]G. Otting, E. Liepinsh, and K. Wuthrich, Science **254**(5034), 974–980 (1991).
[18]K. Wüthrich, M. Billeter, P. Güntert, P. Luginbühl, R. Riek, and G. Wider, Faraday Discuss. **103**, 245–253 (1996).
[19]D. Svergun, S. Richard, M. Koch, Z. Sayers, S. Kuprin, and G. Zaccai, Proc. Natl. Acad. Sci. U. S. A. **95**(5), 2267–2272 (1998).
[20]Y. Levy and J. N. Onuchic, Annu. Rev. Biophys. Biomol. Struct. **35**, 389–415 (2006).
[21]M. Chaplin, Nat. Rev. Mol. Cell Biol. **7**(11), 861–866 (2006).
[22]P. Ball, Cell. Mol. Biol. Paris Wegmann **47**(5), 717–720 (2001).
[23]R. A. Robinson and R. H. Stokes, *Electrolyte Solutions* (Courier Corporation, 2002).
[24]N. Nandi, K. Bhattacharyya, and B. Bagchi, Chem. Rev. **100**(6), 2013–2046 (2000).
[25]S. Mashimo, S. Kuwabara, S. Yagihara, and K. Higasi, J. Phys. Chem. **91**(25), 6337–6338 (1987).
[26]S. Mashimo, S. Kuwabara, S. Yagihara, and K. Higasi, J. Chem. Phys. **90**(6), 3292–3294 (1989).
[27]V. P. Denisov and B. Halle, Faraday Discuss. **103**, 227–244 (1996).
[28]B. Halle, Philos. Trans. R. Soc., B **359**(1448), 1207–1224 (2004).
[29]C. Mattea, J. Qvist, and B. Halle, Biophys. J. **95**(6), 2951–2963 (2008).
[30]S. K. Pal, J. Peon, B. Bagchi, and A. H. Zewail, J. Phys. Chem. B **106**(48), 12376–12395 (2002).
[31]B. Bagchi, *Molecular Relaxation in Liquids* (Oxford University Press, USA, 2012).
[32]T. Li, A. A. Hassanali, Y.-T. Kao, D. Zhong, and S. J. Singer, J. Am. Chem. Soc. **129**(11), 3376–3382 (2007).
[33]S. Mondal, S. Mukherjee, and B. Bagchi, "Decomposition of total solvation energy into core, side-chains and water contributions: Role of cross correlations and protein conformational fluctuations in dynamics of hydration layer," Chem. Phys. Lett. (pulbished online).
[34]F. Sterpone, G. Stirnemann, and D. Laage, J. Am. Chem. Soc. **134**(9), 4116–4119 (2012).
[35]B. Halle and L. Nilsson, J. Phys. Chem. B **113**(24), 8210–8213 (2009).
[36]K. Bhattacharyya, Acc. Chem. Res. **36**(2), 95–101 (2003).
[37]K. Bhattacharyya, Chem. Commun. **2008**(25), 2848–2857.
[38]S. K. Pal, D. Mandal, D. Sukul, S. Sen, and K. Bhattacharyya, J. Phys. Chem. B **105**(7), 1438–1441 (2001).
[39]S. K. Pal, J. Peon, and A. H. Zewail, Proc. Natl. Acad. Sci. U. S. A. **99**(24), 15297–15302 (2002).
[40]D. Zhong, S. K. Pal, D. Zhang, S. I. Chan, and A. H. Zewail, Proc. Natl. Acad. Sci. U. S. A. **99**(1), 13–18 (2002).
[41]K. Furse and S. Corcelli, J. Phys. Chem. Lett. **1**(12), 1813–1820 (2010).
[42]R. Ghosh, S. Banerjee, M. Hazra, S. Roy, and B. Bagchi, J. Chem. Phys. **141**(22), 22D531 (2014).
[43]J. B. Hubbard and P. G. Wolynes, J. Chem. Phys. **69**(3), 998–1006 (1978).
[44]S. Ravichandran and B. Bagchi, Int. Rev. Phys. Chem. **14**(2), 271–314 (1995).
[45]M. Heinig and D. Frishman, Nucleic Acids Res. **32**(suppl 2), W500–W502 (2004).
[46]B. Hess, C. Kutzner, D. Van Der Spoel, and E. Lindahl, J. Chem. Theory Comput. **4**(3), 435–447 (2008).
[47]W. Humphrey, A. Dalke, and K. Schulten, J. Mol. Graphics **14**(1), 33–38 (1996).
[48]W. L. Jorgensen and J. Tirado-Rives, J. Am. Chem. Soc. **110**(6), 1657–1666 (1988).
[49]S. Kirkpatrick, C. D. Gelatt, and M. P. Vecchi, Science **220**(4598), 671–680 (1983).
[50]G. Bussi, D. Donadio, and M. Parrinello, J. Chem. Phys. **126**(1), 014101 (2007).
[51]M. Parrinello and A. Rahman, Phys. Rev. Lett. **45**(14), 1196 (1980).
[52]B. Hess, H. Bekker, H. J. Berendsen, and J. G. Fraaije, J. Comput. Chem. **18**(12), 1463–1472 (1997).
[53]T. Darden, D. York, and L. Pedersen, J. Chem. Phys. **98**(12), 10089–10092 (1993).
[54]B. Jana, S. Pal, and B. Bagchi, J. Chem. Sci. **124**(1), 317–325 (2012).
[55]J. T. King, E. J. Arthur, C. L. Brooks III, and K. J. Kubarych, J. Phys. Chem. B **116**(19), 5604–5611 (2012).
[56]Y. Qin, M. Jia, J. Yang, D. Wang, L. Wang, J. Xu, and D. Zhong, J. Phys. Chem. Lett. **7**(20), 4171–4177 (2016).
[57]B. Bagchi and A. Chandra, J. Chem. Phys. **90**(12), 7338–7345 (1989).
[58]J. G. Kirkwood and J. B. Shumaker, Proc. Natl. Acad. Sci. U. S. A. **38**(10), 855–862 (1952).
[59]M. Neumann, Mol. Phys. **50**(4), 841–858 (1983).
[60]R. J. Smith, D. H. Williams, and K. James, J. Chem. Soc., Chem. Commun. **1989**(11), 682–683.
[61]T. Von Karman and M. A. Biot, *Mathematical Methods in Engineering* (McGraw Hill, 1940).
[62]F. O. Raineri, H. Resat, B. C. Perng, F. Hirata, and H. L. Friedman, J. Chem. Phys. **100**(2), 1477–1491 (1994).
[63]P. Hänggi and H. Thomas, Phys. Rep. **88**(4), 207–319 (1982).
[64]R. Jimenez, G. R. Fleming, P. Kumar, and M. Maroncelli, Nature **369**, 471–473 (1994).
[65]M. Maroncelli, J. Mol. Liq. **57**, 1–37 (1993).
[66]M. Maroncelli, J. Chem. Phys. **94**(3), 2084–2103 (1991).
[67]M. Maroncelli and G. R. Fleming, J. Chem. Phys. **89**(8), 5044–5069 (1988).
[68]B. Bagchi and B. Jana, Chem. Soc. Rev. **39**(6), 1936–1954 (2010).
[69]T. Plakhotnik, E. A. Donley, and U. P. Wild, Annu. Rev. Phys. Chem. **48**(1), 181–212 (1997).
[70]P. G. Debenedetti and F. H. Stillinger, Nature **410**(6825), 259–267 (2001).
[71]E. Limpert, W. A. Stahel, and M. Abbt, BioScience **51**(5), 341–352 (2001).
[72]M. Wilchek, E. A. Bayer, and O. Livnah, Immunol. Lett. **103**(1), 27–32 (2006).
[73]I. H. Segel, *Enzyme Kinetics* (Wiley, New York, 1975).
[74]R. R. Kopito, Trends Cell Biol. **10**(12), 524–530 (2000).
[75]C. A. Ross and M. A. Poirier, Nat. Med. **10**, S10–S17 (2004).
[76]K. Modig, E. Liepinsh, G. Otting, and B. Halle, J. Am. Chem. Soc. **126**(1), 102–114 (2004).